Mine Water and the Environment (2019) 38:757–766
https://doi.org/10.1007/s10230-019-00640-2

TECHNICAL ARTICLE

Investigation of By-products from Acetylene Manufacturing for Acid Mine Drainage Remediation

Sze-Mun Lam[1] · **Jin-Chung Sin**[2]

Received: 19 August 2018 / Accepted: 23 October 2019 / Published online: 29 October 2019

Abstract
We characterized carbide lime, a by-product of acetylene manufacturing, and compared it to commercial calcium oxide (CaO), which is typically used to treat AMD. Chemical and X-ray diffraction data revealed that the carbide lime was a calcium-rich lime. Morphological analysis indicated that it differed from commercial CaO in its morphology, having a layered structure. The presence of functional groups among the samples was confirmed by a Fourier transform infrared spectral study. Physical characterization, including nitrogen adsorption–desorption isotherm and particle size distribution demonstrated that the carbide lime had greater surface area and finer particle size than the commercial CaO. Jar tests were used to evaluate the effect of the carbide lime and CaO loading on actual AMD. The optimum quantity of carbide lime for treating the AMD was 0.4 g/l, which increased the pH and reduced the metal and sulphate concentrations to acceptable levels. The carbide lime showed superior acid-neutralizing and contaminant diminution at all studied loadings. Additionally, an Imhoff cone test confirmed that the sludge produced using carbide lime settled better that that produced using CaO powder.

Keywords Carbide lime · Characterization · Acid mine · Active treatment · Sedimentation test

Introduction

Common treatment techniques for acid mine drainage (AMD) are classified as active and passive processes. The active treatment approaches use chemicals like hydrated lime, caustic soda, limestone, anhydrous ammonia, while passive treatments include biological systems such as constructed wetlands and sulphate-reducing bioreactors, and chemical treatment with limestone (Agrawal and Sahu 2009; Gaikwad and Gupta 2008; Kefeni et al. 2015, 2017; Ochieng et al. 2010; Qureshi et al. 2015; Shabalala et al. 2017; Simmons et al. 2002). Recently, the use of industrial by-products has garnered significant attention since they can be potentially used as alkaline chemicals (Ayeche and Hamdaoui 2012; Cardoso et al. 2009; Kaur et al. 2018). Re-use of such wastes are both economical and ecological.

Carbide lime or lime sludges are by-products of the reaction between calcium carbide in water that are produced during the fabrication of acetylene gas for welding (Cardoso et al. 2009; Chukwudebelu et al. 2013). Based on the statistics of the calcium carbide industry, the global production of calcium carbide was estimated to be 1370 million tons annually (Liu et al. 2011; Zhang et al. 2012). Carbide lime has a pH > 12 and is comprised of 85–95% calcium hydroxide, 10% calcium carbonate, and 1–3% unreacted carbon and silicates (Cardoso et al. 2009; Scott and Wood 2002). They have been identified as non-hazardous but require suitable management prior to disposal. Utilization of the carbide lime as a substitute for lime in construction, agricultural, and other industrial processes have been documented (Hologado et al. 1992; Hower et al. 1998; Scott and Wood 2002). Moreover, they also can be used as alkaline chemicals for dairy farm (Ayeche 2012) and municipal sewage treatment (Ayeche and Hamdaoui 2012), in which they significantly reduced organic matter, suspended solids, nitrogenous, and phosphate compounds.

Electronic supplementary material The online version of this article (https://doi.org/10.1007/s10230-019-00640-2) contains supplementary material, which is available to authorized users.

✉ Sze-Mun Lam
lamsm@utar.edu.my

1 Department of Environmental Engineering, Faculty of Engineering and Green Technology, Universiti Tunku Abdul Rahman, 31900 Kampar, Perak, Malaysia

2 Department of Petrochemical Engineering, Faculty of Engineering and Green Technology, Universiti Tunku Abdul Rahman, 31900 Kampar, Perak, Malaysia

In the present work, calcium carbide lime produced as a by-product of acetylene gas production was evaluated for the treatment of AMD and compared with commercial calcium oxide (CaO). Characterization of the calcium carbide lime was carried out using X-ray fluorescence (XRF), X-ray diffraction (XRD), field emission scanning electron microscope (FESEM), Fourier transform infrared (FTIR) spectroscopy, nitrogen adsorption–desorption, and particle size distribution analyses. Jar tests were used to evaluate the impact of the carbide lime and CaO powder loadings on pH, electrical conductivity (EC), oxidation–reduction potential (ORP), and concentrations of Al, As, Cu, Fe, Mn, Ni, Zn, and sulphate in the AMD. The settling capacities of both AMD sludges were assessed and the particle characteristics was confirmed via FESEM and energy dispersive X-ray (EDX) analyses.

Experimental

Materials

All of the chemical reagents received in this study were analytical grade and used without further purification. Commercially available calcium oxide (CaO) (purity 99%) was purchased from Bendosen Chemical. The carbide lime waste samples were obtained from an acetylene gas plant in Perak, Malaysia (supplemental Fig. S1). Grab sampling was used to obtain the lime waste samples from the plant. The samples were dried in a tray under the sun and then ground with an agate mortar. Subsequently, the particles were segregated using sieves ranging from 45 to 70 mm in the laboratory. The samples were then kept in a desiccator before their use in experiments. The commercial CaO was also segregated using similar sieve sizes prior to the experimental testing.

Acid Mine Water

AMD was obtained from an active tailings pond located in Perak (supplemental Fig. S1). The AMD was analysed using a Perkin Elmer Optima 7000 inductively coupled plasma optical emission spectrometer (ICP–OES) (Table 1). The AMD had a pH of 4.0, which was far below the recommended pH values of 6.0–9.0 and 5.5–9.0 for Malaysia's Environmental Quality Standards A and B, respectively (Environmental Quality Act 1974 (Act 127) & Subsidiary Legislations 1998). In addition, contaminants such as Cu, Fe, Al, As, and Mn were all present at levels that exceeded the maximum acceptable levels permitted by the Environmental Quality Act 1974 (Act 127) & Subsidiary Legislations (1998) and World Health Organization (WHO) (2011).

Table 1 Major chemical content of raw AMD sample collected from Perak, Malaysia

Parameter	Value	Standard A	Standard B	Drinking guideline value
pH	4.0	6.0–9.0	5.5–9.0	6.5–8.5[a]
As (mg/l)	0.8	0.05	0.10	0.01[a]
Cu (mg/l)	16.0	0.20	1.0	2.0[a]
Fe (mg/l)	1.1	1.0	5.0	0.3[b]
Al (mg/l)	20.5	10	15	0.2[b]
Mn (mg/l)	61.8	0.2	1.0	0.1[b]
Ni (mg/l)	10.2	0.2	1.0	0.07[a]
Zn (mg/l)	5.0	2.0	2.0	–

[a]World Health Organisation (WHO)

[b]Department of Water Affairs (DWA), South Africa

Characterization of Carbide Lime

The crystal phase of the samples was tested by X-ray diffraction (XRD) using a Philips PW1820 diffractometer with Cu Kα radiation at a scanning rate of 2° min^{-1} in the range of 20°–70°. The morphology of the samples was monitored by a Quanta FEG 450 field emission-scanning electron microscope (FESEM) with an energy dispersive X-ray (EDX) spectrometer. Prior to this analysis, the sample was prepared on a carbon tape and an auto fine coater was used to coat the samples with thin layer of platinum. The infrared spectrum was completed with a Thermo scientific Nicolet IS10 Fourier Transform Infrared (FTIR) spectrometer at a scanning range from 400 to 4000 cm^{-1}. The specific Brunauer–Emmett–Teller (BET) surface area and pore volume of the samples were assessed by a Micromeritics ASAP 2020 nitrogen adsorption–desorption apparatus. A Shimadzu X-ray fluorescence (XRF-1700) was used to determine the chemical composition of the samples. The particle size distributions were measured by a Malvern Mastersizer 2000 analyser.

Experimental Procedures

Experiments were performed using a VELP Scientifica programmable jar testing apparatus in which 500 ml of AMD was poured into each jar. A proper amount of the solid (0.1–1.6 g/l) with 30–80 µm particles was placed into the AMD. The solution was then mixed at 150 rpm for 1 min, followed by slow mixing at 50 rpm for 5 min and then left to settle for 30 min. After settling, water quality parameters such as pH, EC, and ORP were measured using a Cyberscan PCD650 portable water quality meter. The metal ion analysis of the water samples was tested

Table 2 Chemical composition of commercial CaO and carbide lime measured by XRF analysis

%	Commercial CaO	Carbide lime
CaO	87.69	92.39
SiO_2	3.75	4.30
Al_2O_3	0.96	1.46
Fe_2O_3	0.13	0.69
MgO	5.68	0.29
SO_3	0.12	0.23
C	1.67	0.64
Total	100	100

using an ICP–OES analyser. The sulphate ion analysis was evaluated using an ion chromatography Metrohm 792 Basic IC analyser. For comparison, commercial CaO powder (30–80 µm) was also tested under similar conditions. The settling capacities of sludge volumes after 30 min of sedimentation were assessed using Imhoff cones. Finally, the samples were filtered using vacuum filtration and air dried prior to FESEM and EDX analysis. Each experiment was duplicated and the mean value was reported.

Results and Discussion

Characterization

The main Ca component and other contents such as SiO_2, Fe_2O_3, Al_2O_3, and SO_3 were higher in the carbide lime than in the commercial CaO (Table 2), while the commercial CaO contained more MgO and C than the carbide lime. Thus, the carbide lime can be classified as a Ca-rich lime with low MgO contents. The results agreed well with those reported by Ayeche and Hamdaoui (2012) and Cardoso et al. (2009).

The XRD patterns of commercial CaO and carbide lime are depicted in supplemental Fig. S2. In both cases, major crystalline phases were composed of CaO and $Ca(OH)_2$. A typical peak corresponding to MgO can also be identified in the spectrum for the commercial CaO. The presence of MgO could be mainly due to the nature of the limestones; similar observations were found in the literature (Ontiveros-Ortega

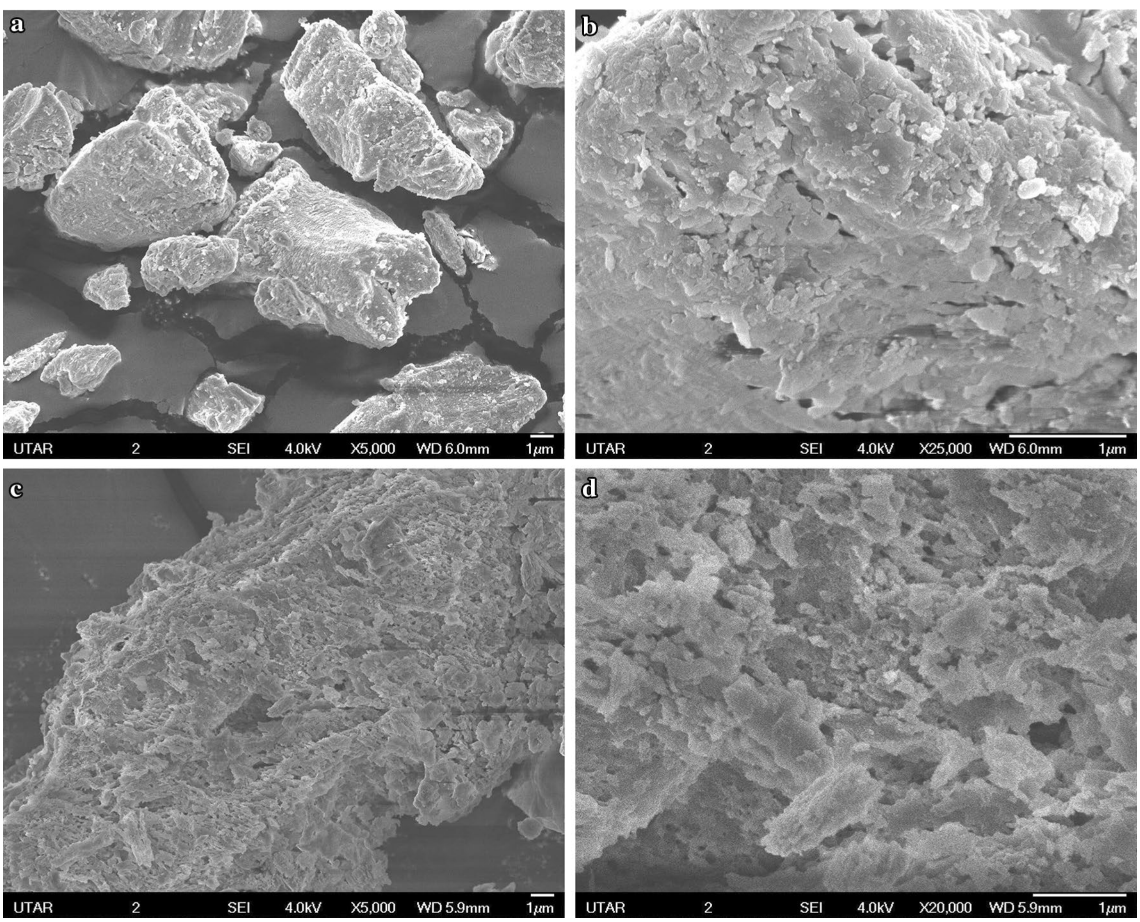

Fig. 1 FESEM images of commercial CaO (**a**, **b**) and carbide lime (**c**, **d**) at different magnifications

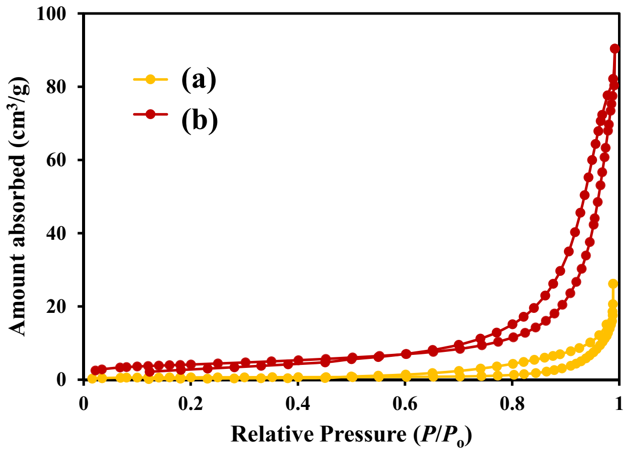

Fig. 2 N_2 adsorption–desorption isotherm of **a** commercial CaO and **b** carbide lime

Table 3 Textural properties of commercial CaO and carbide lime

Material	Surface area (m^2/g)	Pore volume (cm^3/g)
Commercial CaO	4.14	0.0405
Carbide lime	14.82	0.1398

et al. 2017; Rosell et al. 2014). This MgO content could assist in dissolution and its ion exchange during the AMD treatment process. Moreover, the strong and sharp XRD peaks indicated that the both samples were highly crystalline. These properties were well matched with the morphological and textural properties of the samples, as recorded below.

FESEM images of the powder samples at different magnifications are shown in Fig. 1. Figure 1a shows that the commercial CaO particles were granules derived from aggregation of CaO and $Ca(OH)_2$ crystals. The formation of aggregates might be due to the heterogeneous nucleation of these crystals during the sintering process. The magnified image (Fig. 1b) shows that the surface of the aggregates was irregular. These cluster structures were also marked by considerable voids and gaps. From Fig. 1c, d, it is clear that the carbide lime had visibly different microstructures. The carbide lime wastes were also mainly comprised of aggregates, but these were aggregates derived from submicron-sized to micrometer-sized CaO and $Ca(OH)_2$ crystals. These particles were randomly arranged, creating some porous regions and layered textures (Fig. 1d).

The morphological differences between the CaO and $Ca(OH)_2$ clusters were due to their synthesis techniques. The commercial CaO was fabricated by thermal decomposition of calcium carbonate at 800–900 °C to liberate CO_2, leaving fine powder (Ontiveros-Ortega et al. 2017). The CO_2 release that took place produced numerous voids and gaps. In contrast, the carbide lime were produced in an aqueous slurry, followed by filter pressing, and in the current study, also drying and grinding). These reactions produced layered textures with some porosities, which may be beneficial to the solid–liquid interaction during AMD treatment.

FTIR spectra of commercial CaO and carbide lime are depicted in supplemental Fig. S3. The absorption band at 3448 cm^{-1} corresponded to -OH stretching vibration, indicating H_2O bound to the surface of the solid samples. Moreover, the band at 1640 cm^{-1} indicates the adsorption of water on the sample surfaces (Li et al. 2015). The major band at 1459 cm^{-1} is characteristic of Ca–O (Fang et al. 2018). This intense band was observed for the carbide lime,

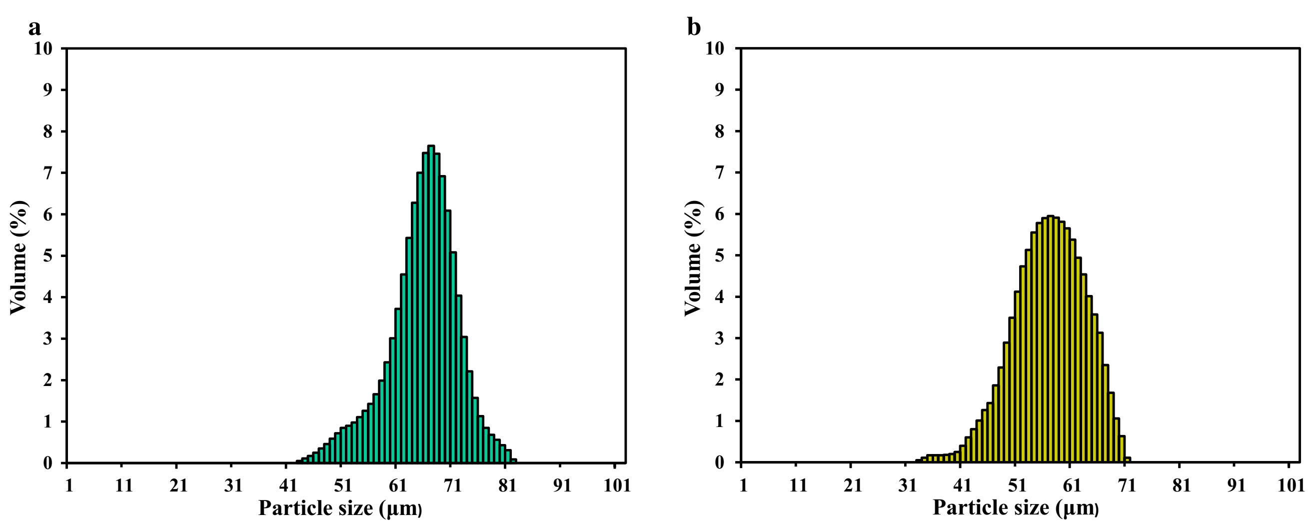

Fig. 3 Particle size distribution of **a** commercial CaO and **b** carbide lime

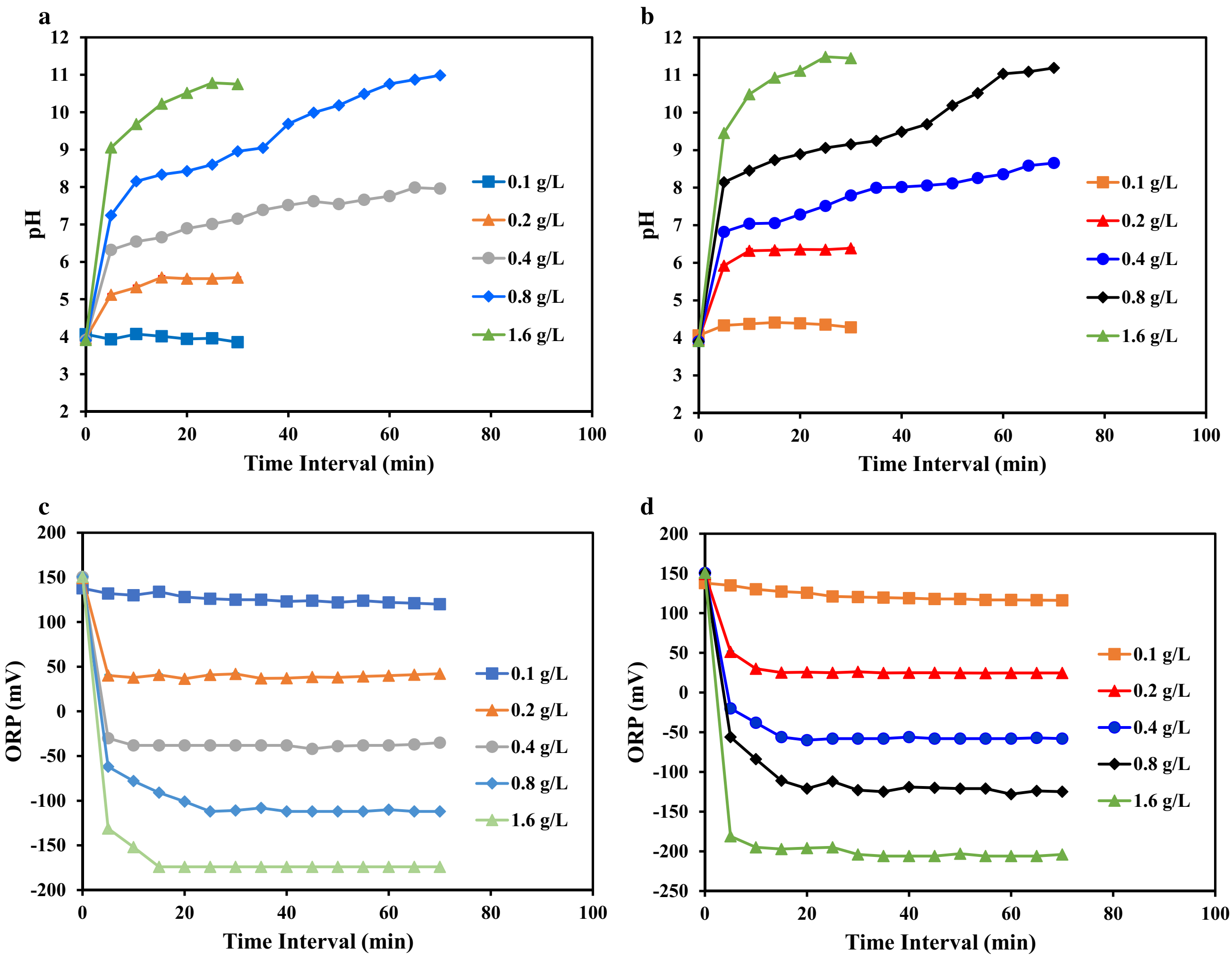

Fig. 4 Solution pH for AMD treated at different loadings of **a** commercial CaO, **b** carbide lime, oxidation reduction potential for AMD treated at varied loadings of **c** commercial CaO and **d** carbide lime

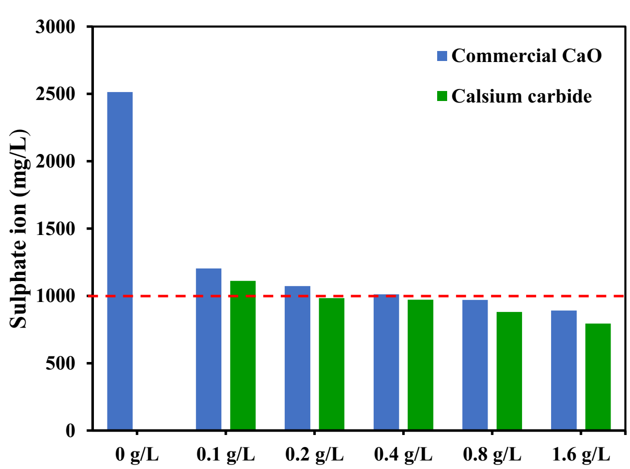

Fig. 5 Sulphate ion analysis for AMD treated using various loadings of commercial CaO and carbide lime

indicating that the sample has the potential to release Ca^{2+} and OH^- ions. In addition, an absorption peak attributed to the Ca–C bond was found at 873 cm^{-1}. The obtained FTIR results were similar to those in the literature (Li et al. 2015; Trubyanov et al. 2018).

The N_2 adsorption–desorption isotherms of the commercial CaO and carbide lime are displayed in Fig. 2. Both samples exhibited type IV isotherms with H3 hysteresis loops. The distinct hysteresis loops were found in the range of 0.6–1.0 P/P_o, which suggested the presence of mesoporous materials. Table 3 summarizes the textural properties established by N_2 physisorption data. The surface area and pore volume of lime wastes were higher than that of the commercial CaO. Surface area can be associated with the morphology, texture, and porosity of particles and to some extent, to their size distributions (Rodriguez-Navarro et al. 2005; Rosell et al. 2014). The much larger specific surface area of the lime wastes could be due to the filter pressing followed

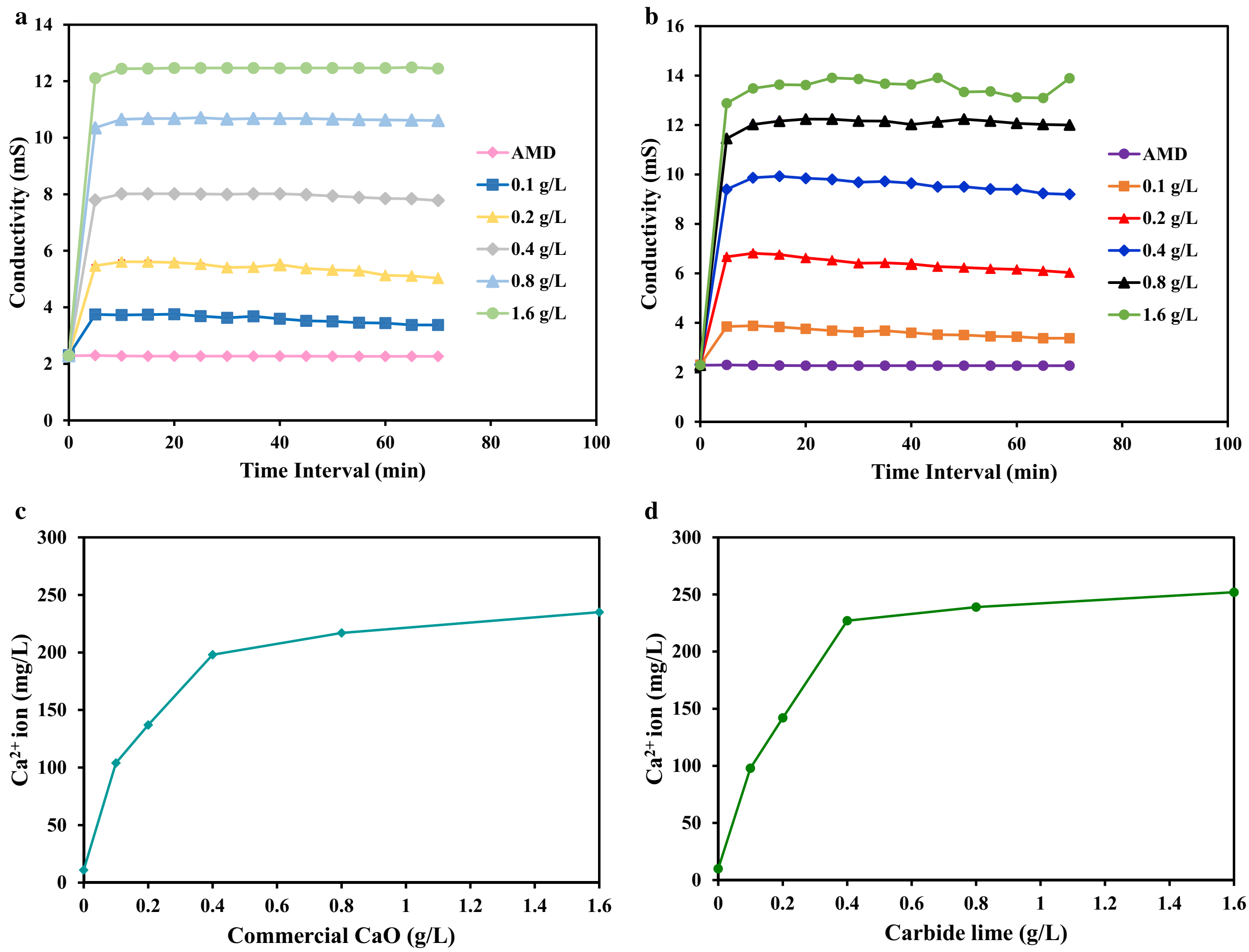

Fig. 6 Electrical conductivity of AMD treated by **a** commercial CaO, **b** carbide lime, Ca concentration treated by **c** commercial CaO and **d** carbide lime

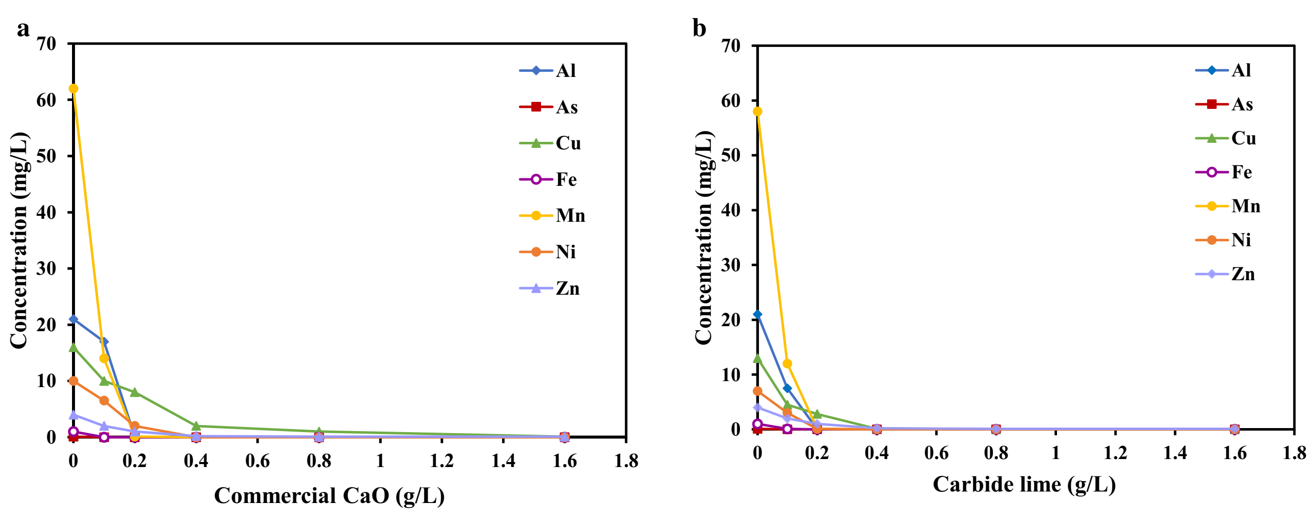

Fig. 7 Metal and metalloid removal at varied loadings of **a** commercial CaO and **b** carbide lime

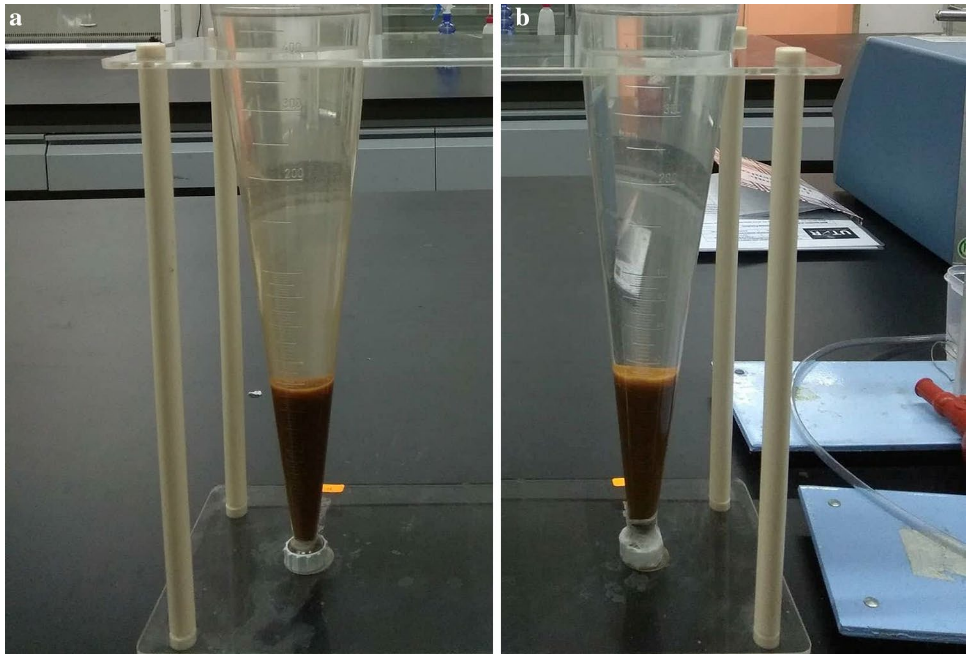

Fig. 8 Assessment in the Imhoff cones **a** commercial CaO and **b** carbide lime

by drying and crushing, creating particle packing and more available surfaces.

Figure 3 depicts the particle size distribution of the commercial CaO and carbide lime. The commercial CaO demonstrated coarse particle with > 10% of large particle size over 75 µm; its median particle size was 65 µm (Fig. 3a). The lime wastes had smaller granulometry. Figure 3b shows that the lime waste particles also had > 10% large particles but its median particle size was 55 µm. The carbide lime used was appropriate to treat AMD effectively due to its fine particle size.

pH and Oxidation–Reduction Potential (ORP)

The chemical form of an element in sulphate-bearing mining waste was significantly affected by physico-chemical boundary conditions, especially with respect to pH and ORP. Figure 4a, b displays the pH of the treated AMD using different loadings of commercial CaO and carbide lime. Both samples showed the same patterns, in that the pH of the treated AMD increased slightly when ≤ 0.2 g/l was applied. Further increasing the sample loadings from 0.4 to 1.6 g/l caused a rapid pH increase. The loading that best met the objective was 0.4 g/l, which complied with both Standard A and B in the Environmental Quality Act 1974. Moreover, the carbide lime powder exhibited better acid neutralization than the commercial CaO at all studied loadings.

Our XRF results indicated a higher CaO content for carbide lime than commercial CaO. Furthermore, when comparing the AMD treatment at different sample loadings, the results suggest that the CaO content of the samples correlated with their pH neutralizing capacities.

The ORP of the AMD at different loadings of commercial CaO and carbide lime was also measured (Fig. 4c, d, respectively). The ORP values changed from oxidizing (positive) to reducing (negative) after treatment, indicating that both samples were able to reduce the ionic chemical species in the AMD. Figure 5 displays the sulphate ion analysis for the treated AMD and indicates that both the commercial CaO and carbide lime were able to lower the sulphate ion concentrations by about 60%.

Metal Concentration and Electrical Conductivity

EC and ICP analyses showed a good relationship between EC and metal concentrations in the AMD. Figure 6a, b shows that the EC increased with greater commercial CaO or carbide lime loading, respectively. Figure 6c, d shows that the Ca concentration in the AMD treated by both samples was obviously higher than that of the untreated AMD. This suggests that dissolution of Ca-bearing alkaline materials was mainly responsible for the EC increase. Furthermore, the higher Ca concentration in the AMD treated with lime wastes led to a larger EC increase, compared to that of commercial CaO. Others have also reported on the increased levels of alkaline components such as Ca and Mg due to dissolution of neutralizing agents in water (Lottermoser 2010; Wang et al. 2008).

Other metal ion concentrations of AMD treated using different loadings of commercial CaO and carbide lime

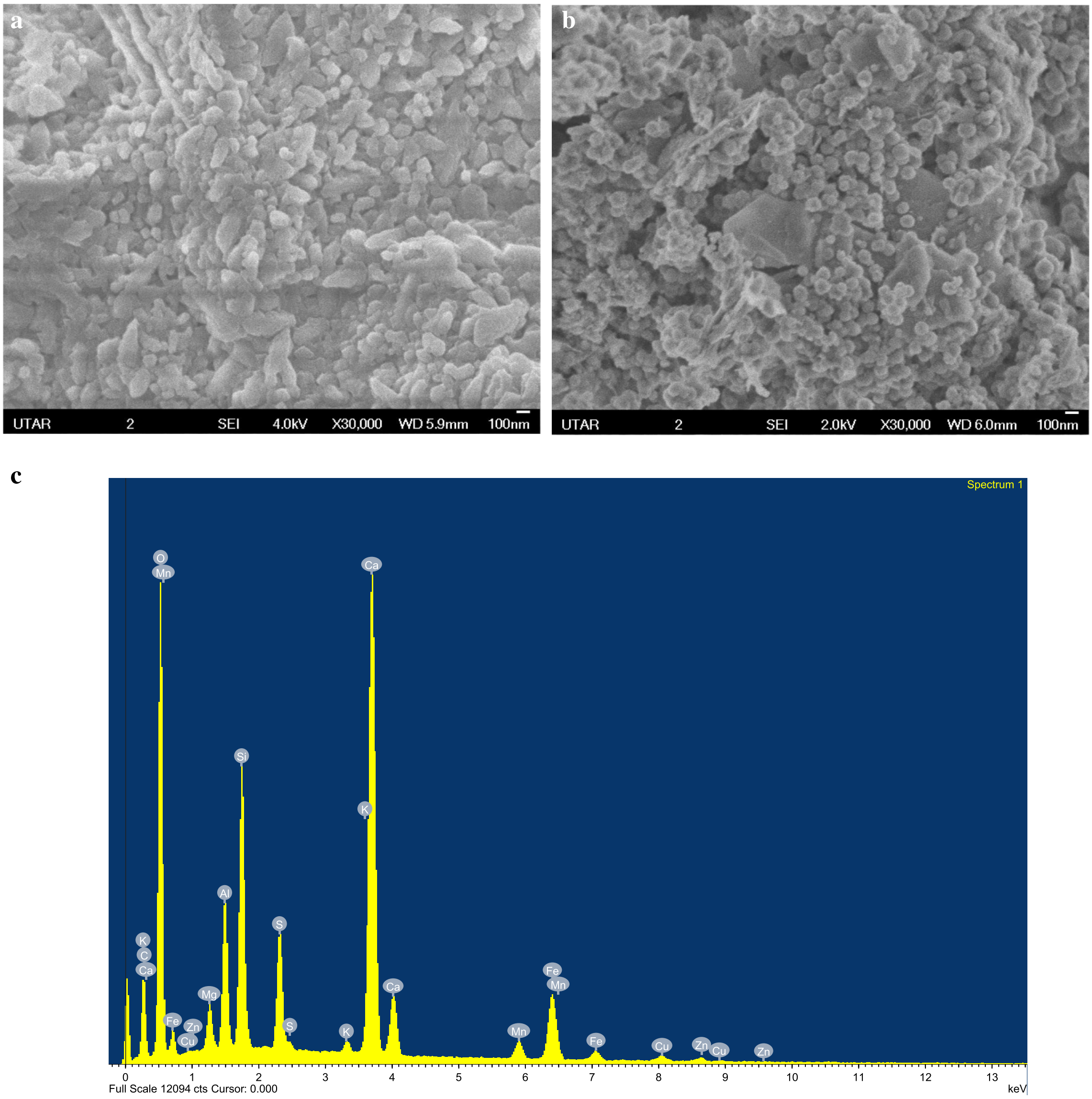

Fig. 9 FESEM images of sludge after completion of the carbide lime with **a** deionized water, **b** AMD and **c** EDX spectrum of treated carbide lime with AMD

are shown in Fig. 7. Both samples showed profound effects in decreasing Al, Cu, Fe, Mn, Ni, and Zn concentrations in AMD when using loadings of 0.4 g/l and above. They reduced these metal ion concentrations in AMD by over 93% and their aqueous concentrations were in compliant with the Environmental Quality Act 1974. Moreover, the samples also reduced As concentrations by 98% and 96%, respectively. The high diminution of the metal and metalloid concentrations was presumably due to precipitation, co-precipitation, and adsorption (because adsorption sites are created as metal hydroxides precipitate).

Settling Efficiency of Sludge

Settling capacities of the sludge produced with commercial CaO and carbide lime in the AMD treatment were compared (Fig. 8). In 30 min of sedimentation, the sludge volume in the carbide lime samples (≈ 28 ml/l) was very similar to the commercial CaO (≈ 25 ml/l). Additionally, the settling capacities of the carbide lime sludge were superior, in that a clear solution was visibly observed for lime wastes.

Microscopic analysis on the produced sludges from carbide lime was conducted using deionized water and AMD solution after the jar test (Fig. 9). The sludge derived from carbide lime with AMD had many abundant clusters of spherical-like precipitates on the surface of lime waste particles compared to that of the sludge derived from deionized water. This confirmed the precipitation of AMD constituents onto the lime waste particles. EDX analysis of the sludge generated by carbide lime treatment of the AMD indicated the presence of various metals including Fe, Mn, Mg, Ca, Cu, and several non-metals such as C, Si, and S. Hence, carbide lime could be an efficient and cost-saving alternative to commercial CaO for AMD remediation.

Conclusion

This work evaluated whether by-products from acetylene production could be used as an alternative to commercial CaO for AMD neutralization. Carbide lime waste was shown to be a Ca-rich lime composed mostly of CaO and $Ca(OH)_2$; a minor quantity of MgO was also identified in the commercial CaO. The carbide lime wastes showed clusters with more open porosities and layered textures than that of commercial CaO, leading to a larger surface area. This was aided by the industry filter-pressing and laboratory preparation methods used for the carbide lime waste samples, which produced a finer particle size distribution than that of commercial CaO. Jar tests were conducted to evaluate the effect of carbide lime and CaO loading on the pH, EC, ORP, and concentrations of Al, As, Cu, Fe, Mn, Ni, Zn, and sulphate anion in the AMD. The optimum application rate of the carbide lime for AMD was 0.4 g/l, which brought the pH and contaminant contaminants into compliance with Standards A and B of the Environmental Act of 1974. The carbide lime also showed superior acid-neutralization and diminution of metals and arsenic than the commercial CaO at all studied loadings. Additionally, sedimentation test in Imhoff cones confirmed that the sludge produced using carbide lime had better settling capacities than that produced using CaO powders for AMD remediation. Hence, carbide lime could be an efficient and cost-saving alternative to commercial CaO for AMD remediation. Long-term tests are currently going on to further understand the stability properties of the solids.

Acknowledgements The research was supported by the Kurita Water and Environment Foundation (KWEF) (Project 17P042). We also thank MCB Industries Sdn. Bhd., especially Q.C./R & D Manager of Mr. Zainal Arif Perwira Bin Zainal Abidin and his staff as well as the staff of the Mineral Research Centre, Minerals and Geoscience Department Perak.

References

Agrawal A, Sahu KK (2009) An overview of the recovery of acid from spent acidic solutions from steel and electroplating industries. J Hazard Mater 171:61–75

Ayeche R (2012) Treatment by coagulation of dairy wastewater with the residual lime of National Algerian Industrial Gases Company (NIGC-Annaba). Energy Procedia 18:147–156

Ayeche R, Hamdaoui O (2012) Valorization of carbide lime waste, a by-product of acetylene manufacture, in wastewater treatment. Desalin Water Treat 50:87–94

Cardoso FA, Fernandes HC, Pileggi RG, Cincotto MA, John VM (2009) Carbide lime and industrial hydrated lime characterization. Powder Technol 195:143–149

Chukwudebelu JA, Igwe CC, Taiwo OE, Tojola OB (2013) Recovery of pure slaked lime from carbide sludge: case study of Lagos State, Nigeria. Afr J Environ Sci Technol 7:490–495

Environmental Quality Act 1974 (Act 127) & Subsidiary Legislations (1998) International law book services

Fang DX, Huang LP, Fang ZY, Zhang Q, Shen QS, Li YM, Xu XY, Jia FY (2018) Evaluation of porous calcium silicate hydrate derived from carbide slag for removing phosphate from wastewater. Chem Eng J 354:1–11

Gaikwad RW, Gupta DV (2008) Review on removal of heavy metals from acid mine drainage. Appl Ecol Environ Res 6:81–98

Hologado MJ, Rives V, Roman SS (1992) Thermal decomposition of $Ca(OH)_2$ from acetylene manufacturing: a route to supports for methane oxidative coupling catalysts. J Mater Sci Lett 11:1708–1710

Hower JC, Graham U, Wong AS (1998) Influence of flue-gas desulfurization systems on coal combustion by-product quality at Kentucky power stations burning high sulfur coal. Waste Manag Res 17:523–533

Kaur G, Couperthwaite SJ, Hatton-Jones BW, Millar GJ (2018) Alternative neutralisation materials for acid mine drainage treatment. J Water Proc Eng 22:46–58

Kefeni KK, Msagati TAM, Maree JP, Mamba BB (2015) Metals and sulphate removal from acid mine drainage in two steps via ferrite sludge and barium sulphate formation. Miner Eng 81:79–87

Kefeni K, Msagati TAM, Mamba BB (2017) Acid mine drainage: prevention, treatment options, and resource recovery: a review. J Clean Prod 151:475–493

Li FJ, Li QH, Wang LG, Cao Y (2015) Waste carbide slag as a solid base catalyst for effective synthesis of biodiesel via transesterification of soybean oil with methanol. Fuel ProcTechnol 131:421–429

Liu XY, Zhua B, Zhou WJ, Hua SY, Chen DJ, Griffy-Brown C (2011) CO_2 emissions in calcium carbide industry: an analysis of China's mitigation potential. Int J Greenh Gas Control 5:1240–1249

Lottermoser B (2010) Mine wastes: characterization, treatment and environmental impacts, 3rd edn. Springer, Berlin

Ochieng GM, Seanego ES, Nkwata OI (2010) Impacts of mining on water resources in South Africa: a review. Sci Res Essays 5:3351–3357

Ontiveros-Ortega E, Ontiveros-Ortega A, Moleon JA, Ruiz-Agudo E (2017) Electrokinetic and thermodynamic characterization of lime-water interface: physical and rheological properties of lime mortar. Constr Build Mater 151:809–818

Qureshi A, Maurice C, Ohlander B (2016) Potential of coal mine waste rock for generating acid mine drainage. J Geochem Explor 160:44–54

Rodriguez-Navarro C, Ruiz-Agudo E, Ortega-Huertas M, Hansen E (2005) Nanostructure and irreversible colloidal behavior of $Ca(OH)_2$: implications in cultural heritage conservation. Langmuir 21:10948–10957

Rosell JR, Haurie L, Navarro A, Cantalapiedra IR (2014) Influence of the traditional slaking process on the lime putty characteristics. Constr Build Mater 55:423–430

Scott A, Wood A (2002) Pigments-making PCC from carbide lime waste. Chem Week 164:28

Shabalala AN, Ekolua SO, Diop S, Solomon F (2017) Pervious concrete reactive barrier for removal of heavy metals from acid mine drainage-column study. J Hazard Mater 323:641–653

Simmons J, Ziemkiewics P, Courtney Black D (2002) Use of steel slag leach beds for the treatment of acid mine drainage. Mine Water Environ 21:91–99

Trubyanov MM, Mochalov GM, Suvorov SS, Puzanov ES, Petukhov AN, Vorotyntsev IV, Vorotyntsev VM (2018) Towards the interaction between calcium carbide and water during gas-chromatographic determination of trace moisture in ultra-high purity ammonia. J Chromatogr A 1560:71–77

Wang J, Wang T, Burken J, Chusuei C, Ban H, Ladwig K, Huang C (2008) Adsorption of arsenic (V) onto fly ash: a speciation-based approach. Chemosphere 72:381–388

World Health Organization (WHO) (2011) Guidelines for drinking-water quality, 4th edn. World Health Organisation, Malta

Zhang WY, Hu Y, Xi LJ, Zhang YJ, Gu HC, Zhang T (2012) Preparation of calcium carbonate superfine powder by calcium carbide residue. Energy Procedia 17:1635–1640